Research paper

ACE2 expression in rat brain: Implications for COVID-19 associated neurological manifestations

Vito S. Hernández [a],[1], Mario A. Zetter [a],[1], Enrique C. Guerra [a], Ileana Hernández-Araiza [a],[b], Nikita Karuzin [a],[c], Oscar R. Hernández-Pérez [a], Lee E. Eiden [d], Limei Zhang [a],[*]

[a] *Dept. Physiology, Laboratory of Systems Neuroscience, School of Medicine, National Autonomous University of Mexico (UNAM, Mexico City, Mexico)*
[b] *School of Medicine University of Maryland, Baltimore, MD, USA*
[c] *School of Medicine, Pan-American University, Mexico City, Mexico*
[d] *Section on Molecular Neuroscience, NIMH-IRP, NIH, Bethesda, MD, USA*

ARTICLE INFO

ABSTRACT

We examined cell type-specific expression and distribution of rat brain angiotensin-converting enzyme 2 (ACE2), the receptor for SARS-CoV-2, in the rodent brain. ACE2 is ubiquitously present in brain vasculature, with the highest density of ACE2 expressing capillaries found in the olfactory bulb, the hypothalamic paraventricular, supraoptic, and mammillary nuclei, the midbrain substantia nigra and ventral tegmental area, and the hindbrain pontine nucleus, the pre-Bötzinger complex, and nucleus of *tractus solitarius*. ACE2 was expressed in astrocytes and astrocytic foot processes, pericytes and endothelial cells, key components of the blood-brain barrier. We found discrete neuronal groups immunopositive for ACE2 in brainstem respiratory rhythm generating centers, including the pontine nucleus, the parafascicular/retrotrapezoid nucleus, the parabrachial nucleus, the Bötzinger, and pre-Bötzinger complexes and the nucleus of tractus solitarius; in the arousal-related pontine reticular nucleus and gigantocellular reticular nuclei; in brainstem aminergic nuclei, including substantia nigra, ventral tegmental area, dorsal raphe, and locus coeruleus; in the epithalamic habenula, hypothalamic paraventricular and supramammillary nuclei; and in the hippocampus. Identification of ACE2-expressing neurons in rat brain within well-established functional circuits facilitates prediction of possible neurological manifestations of brain ACE2 dysregulation during and after COVID-19 infection.

1. Introduction

The angiotensin-converting enzyme ACE2 (EC 3.4.15.1) is a metalloproteinase discovered in 2000 by two independent groups (Donoghue et al., 2000; Tipnis et al., 2000). Since then, it has been characterized as a counterregulatory component for the classical renin-angiotensin-aldosterone system (RAAS), responsible for cleaving angiotensins I and II to peptides (angiotensin (1–9) and (1–7), respectively) whose effects oppose the vasoconstrictor/proinflammatory actions of angiotensins generated by angiotensin-converting enzyme (ACE) (Rice et al., 2004) (Zhang et al., 2021). Moreover, the ability of ACE2 to hydrolyze other peptides such as apelin, kinins, (des-Arg9)-bradykinin, neurotensin, and dynorphin A-(1−13) (Vickers et al., 2002) provide additional complexity to the roles of ACE2 in RAAS counter-regulation, and

association with various diseases pathophysiology.

SARS-CoV-2, the pathogen of the current COVID-19 pandemic, is associated with the RAAS (Zhang et al., 2021). The virus uses ACE2 as a receptor to invade cells by binding to it via the viral trimeric spike protein (Yan et al., 2020). The spike protein is primed by the serine protease TMPRSS2, triggering the fusion of viral and cellular membranes and internalizing both virus and receptor in the first step of cellular infection (Zhang et al., 2020).

The acute and chronic neurological manifestations of COVID-19, such as headache, dizziness, loss or disruption of the sense of smell (anosmia/dysosmia), taste (ageusia/dysgeusia), loss of muscular coordination (ataxia), loss of autonomic respiratory control, lethargy, depression, and anxiety (Kabbani and Olds, 2020, Mao et al., 2020, Satarker and Nampoothiri, 2020, Haidar et al., 2021, Nagu et al., 2021,

Stefano et al., 2021), as well as its potential contribution to long-term adverse cerebrovascular, neuropsychiatric, and neurodegenerative pathologies (Cohen et al., 2020, Ding et al., 2021, Nagu et al., 2021, Rahman et al., 2021) (Sashindranath and Nandurkar, 2021) are still poorly understood. Thus, there is an urgent need to determine brain ACE2 expression at the cellular and regional levels and analyze its potential participation in defined functional circuits associated with the neurological manifestations of COVID-19.

Here, we examined cell type-specific expression and regional distribution of ACE2 in the rodent brain. We used immunohistochemistry to characterize the pattern of ACE2 expression in vascular, glial, and neuronal elements, participants of several well-defined circuits for respiratory rhythm, arousal, reward, homeostasis, learning, and memory. We analyze and discuss the possible consequences of the disruption of these circuits in contributing to COVID-19 CNS disease.

2. Material and methods

2.1. Animals and brain section preparation

Four male Wistar rats from the local animal breeding facility were used in the present study. Animals were housed with two other littermates, food and water ad libitum, temperature maintained between 20 °C and 25 °C, artificial illumination established to light-on at 8:00 h., and light-off at 20 h., and bedding changed three times per week. For immunohistochemistry, rats were deeply anesthetized with pentobarbital 63 mg/kg; when eyelid reflex was abolished, the animals were perfused transcardially with 0.9% NaCl solution followed by 0.1 M phosphate buffer (PB, pH 7.4) containing 4% paraformaldehyde and 15% *v*/v of a saturated picric acid solution. The brains were quickly removed and thoroughly washed with PB. Sagittal 70 μm sections through the whole mediolateral span were obtained with a vibratome (Leica VT1000S, Germany). All animals were handled according to the guidelines and requirements of the National Institutes of Health Guide for the Care and Use of Laboratory Animals (8th edition) and the Mexican Official Norm for Use, Care and Reproduction of Laboratory Animals (NOM-062-ZOO-1999). Experimental protocols were reviewed and approved by the local Research and Ethics Committee (CIEFM-062-2016).

2.2. Immunohistochemistry

For immunoperoxidase staining for ACE2, sagittal serial sections (at intervals of 140 μm) were selected from two rats. Sections were first blocked against unspecific labeling through incubation in 10% normal donkey serum (NDS) in 0.05 M Trizma buffer, with 0.9% NaCl and 0.3% Triton X-100 (TBST), at room temperature (RT) for two hours. Primary antibody rabbit anti-ACE2 (ab15348, 1:1000, Abcam, MA, USA, see also Table 1 for antibody information) was used, diluted in TBST +1% NDS during 48 h at 4 °C with gentle shaking. After being washed with TBST, sections were incubated with a peroxidase-conjugated donkey anti-rabbit IgG (Jackson Immunoresearch, 711–035-152, PA, USA) for 2 h. at RT. Sections were washed with 0.1 M PB, and immunoreaction was chromogenically developed using 3,3′-diaminobenzidine (Sigma-Aldrich, D5637, MO, USA) and H_2O_2 as substrates. Negative control sections were processed without adding the primary antibody. Finally, slices were mounted on glass slides, dehydrated with ethanol, transferred to xylene, and cover-slipped using Permount mounting medium. (Fischer Chemical, SP15–100, MA, USA).

For multi-channel immunofluorescence staining, sections adjacent to those processed for chromogenic reaction were selected and incubated with 10% normal donkey serum in TBST for two hours at RT. After this blocking step, sections were incubated for 48 h at 4 °C with cocktails of primary antibodies against ACE2 and combinations of the following markers: calretinin (CR, a calcium-binding protein with a high expression in several nuclei of the brainstem and the olfactory bulb); the

Table 1
Primary and secondary antibodies.

Primary antibodies	Host species	Dilution	Source	Source code
Polyclonal IgG anti-Angiotensin converting enzyme type 2 (ACE2)	Rabbit	1:1000	Abcam, MA, USA (www.abcam.com)	ab15348 Lot. GR-3333640-6
Monoclonal IgG anti-Calretinin (CR)	Mouse	1:1000	Swant, Marly Switzerland (www.swant.com)	6B3
Polyclonal IgG anti-Glycine Transporter 2 (GlyT2)	Guinea pig	1:1000	Frontier Institute, Japan (nittobo-nmd.co.jp/)	AF880
Polyclonal IgG anti-Tyrosine Hydroxylase	Sheep	1:2000	Chemicon-Millipore, CA, USA (www.merckmillipore.com)	AB1542
Polyclonal IgG anti-Tryptophan Hydroxylase (TPH)	Sheep	1:2000	Chemicon-Millipore, CA, USA (www.merckmillipore.com)	AB1541
Polyclonal IgG anti-AVP-neurophysin-specific	Mouse	1:1000	Kind gift from Prof. Harold Gainer, National Institute of Mental Health NIH, MD, USA	PS-41
Monoclonal IgG anti-Neuron-Specific Nuclear Protein (NeuN)	Mouse	1:1000	Chemicon-Millipore, CA, USA (www.merckmillipore.com)	MAB377
Monoclonal IgG anti-Glial Fibrillary Acidic Protein (GFAP).	Mouse	1:1000	Biocare Medical, CA, USA (biocare.net/)	CM065A
Polyclonal IgG Anti-von Willebrand Factor (vWF)	Sheep	1:1000	Abcam, MA, USA (www.abcam.com)	ab11713 Lot. GR-3197929-13
Secondary antibodies	Host species	Dilution	Source	Source code
Peroxidase conjugated anti-Rabbit IgG	Donkey	1:500	Jackson Immunoresearch, PA, USA (https://www.jacksonimmuno.com/)	711–035-152
Alexa Fluor 488 anti-Rabbit IgG	Donkey	1:500	Jackson Immunoresearch, PA, USA (https://www.jacksonimmuno.com/)	711–545-152
Alexa Fluor 594 anti-Mouse IgG	Donkey	1:500	Jackson Immunoresearch, PA, USA (https://www.jacksonimmuno.com/)	715–585-150
DyLight 405 anti-Guinea Pig	Donkey	1:500	Jackson Immunoresearch, PA, USA (https://www.jacksonimmuno.com/)	706–475-148
Alexa Fluor 633 anti-Sheep	Donkey	1500	ThermoFisher Scientific, MA, USA (www.thermofisher.com)	A21100

glycine transporter 2 (GlyT2, a marker of glycinergic neurons, highly expressed in the pontomedullary region of the brain); tyrosine hydroxylase (TH, a marker for catecholaminergic neurons), tryptophan hydroxylase (TPH, a marker for serotoninergic neurons); AVP-neurophysin (a marker for vasopressinergic neurons); neuron-specific nuclear protein (NeuN, a pan-neuronal marker); von Willebrand Factor (vWF, a marker for endothelial cells) and glial fibrillary acidic protein (GFAP, a marker for astrocytes). See Table 1 for details about the antibodies used in this study. After primary antibody incubation, the sections were washed

three times in TBST and incubated with the corresponding secondary antibodies (see Table 1). Finally, sections were washed thoroughly in TBS and mounted on glass slides with Vectashield antifade mounting medium (Vector, H1000, CA, USA). The DAB-developed slices were observed with an Olympus CX31 light microscope. Panoramic reconstructions of chromogenic developed sections were obtained with a Zeiss AxioZoom V.16 microscope. Fluorescent images were obtained using a Zeiss confocal LSM 880.

2.3. Quantification of ACE2 expression by optical intensity measurement in immunofluorescence photomicrographs

Using the whole-brain digitally scanned images of the chromogenically developed slides, we identified regions of high vascularization. A confocal fluorescence image was obtained from similar regions in the adjacent sections that were processed for immunofluorescence. Laser intensity, Airy disk diameter, detector gain, offset, and exposure time parameters were fixed between photomicrographs. Images were obtained in an 8bit format. Thus the possible values for each pixel ranged from "0" (no light) to "255" (maximum possible value). To calculate the optical intensity (O.I.) from the light emitted at a determined region of interest (ROI), the average O.I. of the pixels in a square 2500 μm^2 area within the ROI was measured with the program ZEN lite 3.1 (Carl Zeiss

Microscopy GmbH, Germany). The average O.I. value of the background was calculated from five regions with no tissue, thus only obtaining the value from the glass slide and mounting medium. This background value was subtracted from the value obtained in the ROIs. Finally, O.I. values were standardized, assigning 10 relative fluorescence intensity units to the main olfactory bulb (the region with the highest measured O.I.).

3. Results

3.1. General expression pattern of ACE2

The initial evaluation of ACE2 immunoreactivity through the rat brain was performed in peroxidase-DAB developed slices (Fig. 1). High expression of ACE2 was observed in capillaries throughout the brain, with the highest expression in the glomerular layer of the main olfactory bulb (MOBgl). Other regions with a high density of ACE2 expressing vessels were the supraoptic (SON), paraventricular (PVN), and mammillary (MM) nuclei of the hypothalamus; the lateral habenula (LHb) in the epithalamus; the *substantia nigra* (SN) and ventral tegmental area (VTA) in the mesencephalon; and the nucleus of tractus solitarius (NTS), gigantocellular reticular nucleus (GRN), pontine nucleus (PN), pontine reticular nucleus (PRN), pre-Bötzinger complex (pre-BötC) and Bötzinger complex within the pontomedullary region. ACE2 expression
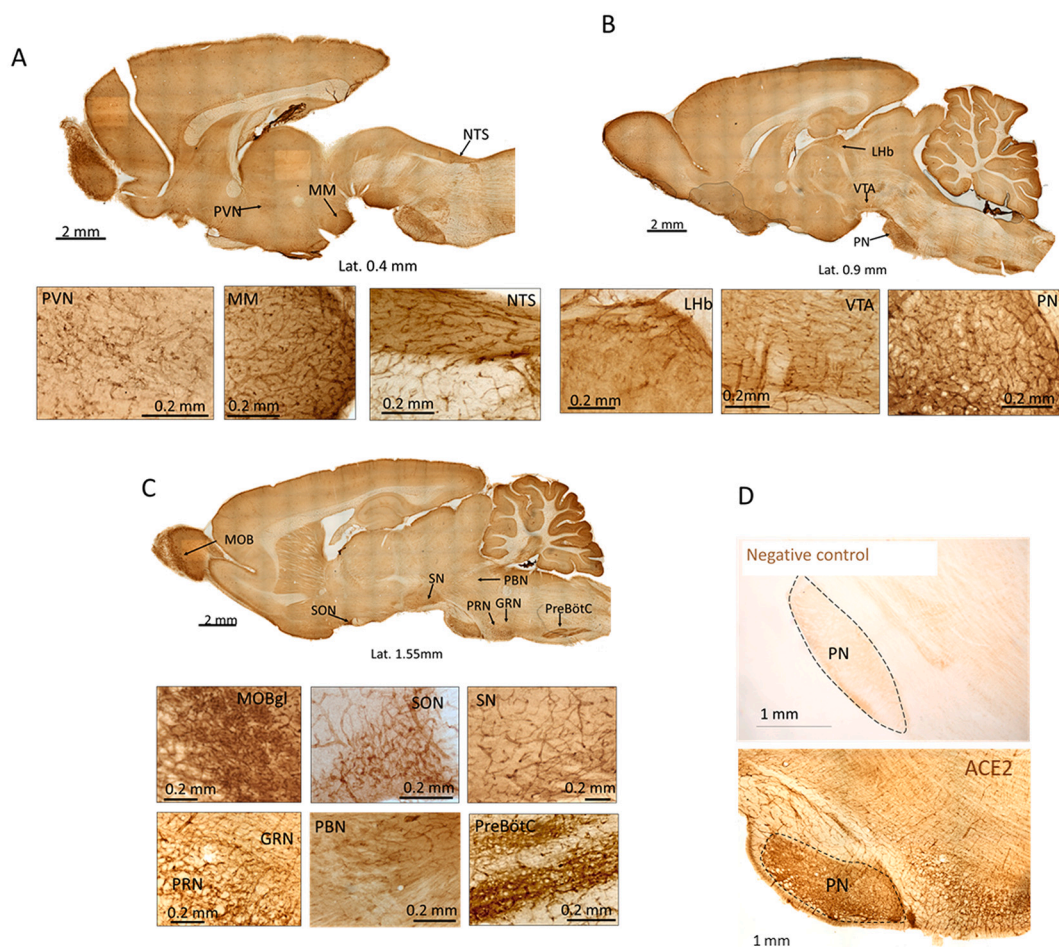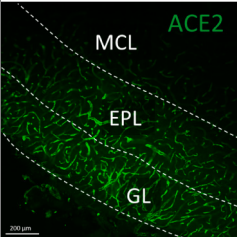

Fig. 1. ACE2 expression in the whole rat brain. A-C: Scanned photomicrographs of representative sections immunoreacted against ACE2 at three mediolateral coordinates. High expression of ACE2 was observed in the vasculature of the glomerular layer of the main olfactory bulb (MOBgl, panel C), paraventricular hypothalamic (PVN, panel A) and supraoptic (SON, panel C) nuclei, mammillary nucleus (MM, panel A), lateral habenula (LHb, panel B), ventral tegmental area (VTA, panel B), substantia nigra (SN, panel C), pontine nucleus (PN, panel B), pontine reticular nucleus (PRN, panels C), gigantoreticularis nucleus (GRN, panels C), parabrachial nucleus (PB, panel C), pre-Bötzinger complex (PreBötC, panel C), and nucleus of the tractus solitarius (NTS, panel A). D. top panel shows the negative control of the immunohistochemistry comparing with the positive control (low panel).

Table 2
ACE2 immunoreactivity in richly vascularized regions of rat brain.

Region	RFI unit*
Telencephalon	

Region	RFI unit*
Telencephalon	
Main olfactory bulb	4.1
• mitral cell layer (MCL)	7.35
• external plexiform layer (EPL)	10
• glomerular layer (MOBgl)	
Diencephalon	
Lateral habenula (LHb)	7.64
Mammillary bodies (MM)	9.23
Paraventricular nucleus (PVN)	8.41
Supraoptic nucleus (SON)	9.92
Suprammamillary nucleus (SUM)	7.08
Mesencephalon	
Dorsal raphe (DR)	6.99
Interpeduncular nucleus (IP)	7.19
Sustantia nigra (SN)	8.52
Ventral tegmental area (VTA)	8.76
Pontomedullary region	
Gigantocellular reticular nucleus (GRN)	8.26
Locus coeruleus (LC)	6.32
Nucleus of tractus solitarius (NTS)	8.94
Parabrachial nucleus (PBN)	7.01
Pontine nucleus (PN)	8.80
Pontine reticular nucleus (PRN)	8.14
Pre-Bötzinger complex (pre-BötC)	8.44
Bötzinger complex (BötC)	8.82
Retrotrapezoid nucleus (RTN)	6.48

* RFI: values are expressed in relative fluorescence intensity units *(*RFI units) and correspond to the mean of the emitted light intensity for each region, on a scale going from "0" (0 light emitted) to "10" (top intensity assigned from the mean value in the glomerular layer of the main olfactory bulb). See method section for technical details

Table 2 (*continued*)

Region	RFI unit*
• mitral cell layer (MCL)	7.35
• external plexiform layer (EPL)	10
• glomerular layer (MOBgl)	
Diencephalon	
Lateral habenula (LHb)	7.64
Mammillary bodies (MM)	9.23
Paraventricular nucleus (PVN)	8.41
Supraoptic nucleus (SON)	9.92
Suprammamillary nucleus (SUM)	7.08
Mesencephalon	
Dorsal raphe (DR)	6.99
Interpeduncular nucleus (IP)	7.19
Sustantia nigra (SN)	8.52
Ventral tegmental area (VTA)	8.76
Pontomedullary region	
Gigantocellular reticular nucleus (GRN)	8.26
Locus coeruleus (LC)	6.32
Nucleus of tractus solitarius (NTS)	8.94
Parabrachial nucleus (PBN)	7.01
Pontine nucleus (PN)	8.80
Pontine reticular nucleus (PRN)	8.14
Pre-Bötzinger complex (pre-BötC)	8.44
Bötzinger complex (BötC)	8.82
Retrotrapezoid nucleus (RTN)	6.48

*RFI: values are expressed in relative fluorescence intensity units (*RFI* units) and correspond to the mean of the emitted light intensity for each region, on a scale going from "0" (0 light emitted) to "10" (maximum intensity assigned from the mean value in the glomerular layer of the main olfactory bulb). See method section for technical details.

was quantified by measuring the relative fluorescence intensity (*RFI*) in photomicrographs obtained from adjacent slices from the regions shown and processed for ACE2 immunofluorescence (Table 2).

3.2. ACE2 expression in identified cells of the blood-brain barrier

Through GFAP immunoreaction and confocal microcopy assessment, we determined the expression of ACE2 in astrocytes throughout the brain. Some of those immunopositive cells were found extending their end-feet processes to surrounding blood vessels (Fig. 2A) or in close contact with the soma of neuronal bodies (Fig. 8). All identified pericytes also expressed ACE2, and some endothelial cells labeled with the antibody against vWF also expressed ACE2 (Fig. 2B).

3.3. ACE2 expression in brainstem arousal and respiratory networks

In the pontomedullary region, we found a high expression of ACE2 in the neuropil and in cells of the neurovascular unit clustered in nuclei that belong to the brainstem respiratory network (Fig. 3A). The nuclei where most of the ACE2 positive cells were observed were the parabrachial nucleus (PBN), the nucleus of tractus solitarius (NTS), pre-Bötzinger complex (pre-BötC), retrotrapezoid nucleus (RTN), and Bötzinger complex. In the pre-BötC, some of those neurons were further characterized as glycinergic, expressing the glycine transporter type 2 ((GlyT2 immunopositive), Fig. 3, inset of panel E).

In the arousal-related reticular formation, a high density of ACE2 positive cells was also found, especially in the pontine reticular nucleus (PRN) and gigantocellular reticular nucleus (GRN) (see Fig. 4).

3.4. ACE2 expression in catecholaminergic and serotoninergic nuclei related to reward, movement, and motivation networks

High ACE2 expression was observed in brainstem regions that contain dopaminergic, noradrenergic, and serotoninergic neurons. Fig. 5 shows examples of ACE2-positive cells expressing tyrosine hydroxylase (TH), the rate-limiting enzyme for the synthesis of dopamine and noradrenaline or tryptophan hydroxylase (TPH) enzyme for the synthesis of serotonin. Double TH+ ACE2+ cells were found in the dopaminergic substantia nigra pars compacta (SNc, panels B) and

ventral tegmental area (VTA, panels C) regions and in the noradrenergic region of locus coeruleus (LC). At the mediolateral level 0.18 mm examined within the dorsal raphe (DR, panels E), we found a high density of TPH neurons co-expressing ACE2, the glycine transporter 2 (GlyT2), and calretinin (CR, a calcium-binding protein); however, we also found sparse TPH+ neurons that were negative for ACE2 and did not express GlyT2 or CR.

3.5. ACE2 in diencephalic homeostatic networks

Compared to pontomedullary or mesencephalic ACE2 expression, lower ACE2 immunoactivity was observed in the diencephalon. However, we identified cells expressing ACE2 in the epithalamic lateral habenula (LHb) and the hypothalamic paraventricular (PVN), supraoptic (SON), and supramammillary (SUM) nuclei (Fig. 6). The lateral habenula, a key modulator of the aminergic centers of the midbrain, hosted a significant number of ACE2 positive for CR (Fig. 6, panels Bs). In PVN, most of the vasopressin (AVP) expressing neurons co-express ACE2 (Fig. 6, panels Cs). In the SUM, ACE2 expression was observed in TH-positive neurons, but not in other NeuN-positive cells (Fig. 6, panels Ds).

3.6. Expression of ACE2 in cognitive networks

The hippocampus has a high expression of ACE2 in astrocytes and some neurons mainly located below the principal cell layers of CA1 and CA2. Astrocytic processes containing ACE2 appear to contact the soma of the principal neurons in all of these layers. Fig. 7 shows the three Cornu Ammonis (CA) areas with white arrows indicating identified interneurons expressing ACE2 and yellow arrows indicating the GFAP-expressing astrocytes close to the neuronal principal layer.

3.7. Expression of ACE2 in the main olfactory bulb

The olfactory bulb is one of the regions with the highest expression of ACE2, especially in the glomerular layer (MOBgl) (Table 2). We investigated ACE2 co-expression with TH or CR, molecules known to be expressed in the glomerular layer. We found that ACE2 is expressed in TH-positive but not CR-positive neurons in MOB (Fig. 8).
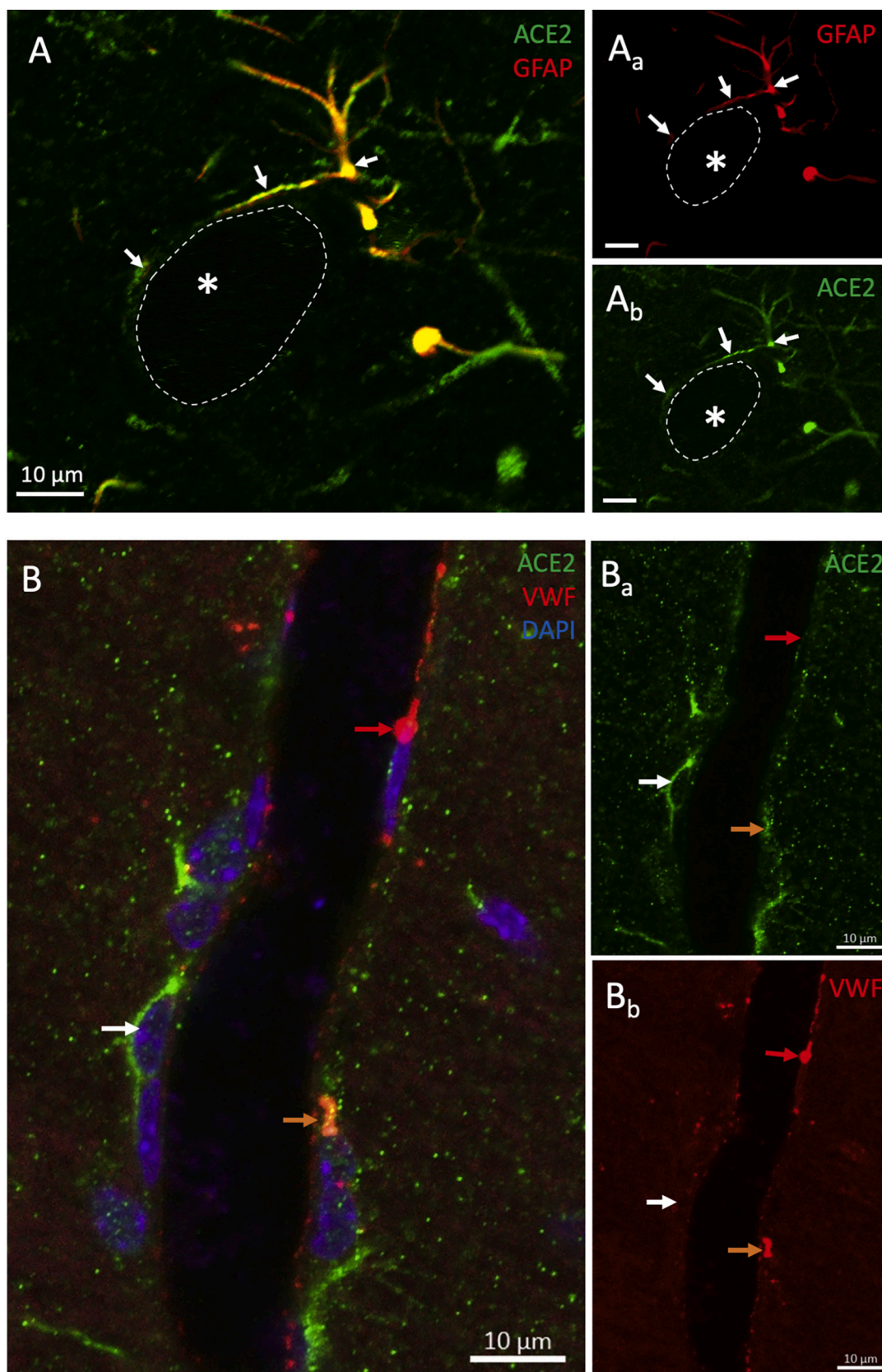
Fig. 2. ACE2 is expressed in the components of the blood-brain barrier. A) Confocal micrographs show an astrocyte (GFAP labeling) positive for ACE2. Notice the ACE2 positive astrocytic processes surrounding a blood vessel delineated by dotted lines. B) Photomicrograph shows the expression of ACE2 in a pericyte (white arrow) and an endothelial cell labeled for vWF (orange arrow). A red arrow indicates an ACE2 negative endothelial cell. (For interpretation of the references to colour in this figure legend, the reader is referred to the web version of this article.)

4. Discussion

In this study we report a widespread expression of ACE2 immunoreaction through the rat brain in a cell type and anatomical regional-specific manner. It is particularly remarkable that in the brain vasculature, the constituent elements for the blood-brain barrier all expressed ACE2, with a particularly high density of immunopositive vasculatures in the olfactory bulb, the hypothalamic nuclei, the midbrain dopaminergic regions, and in various brainstem respiratory nuclei associated with breathing regulation and arousal. Co-expression of ACE2 with other molecular signatures in localized groups of neurons, participants of several well-defined circuits, such as respiratory rhythm, arousal, reward, homeostasis, learning, and memory, are described in detail. The potential impairment of these structures could be the neural substrate for the clinical manifestations of COVID-19 and the post-acute COVID-19 syndrome.

The expression of ACE2 in different tissues and organs has been associated with the maintenance of diverse physiological processes, for instance, regulating cell survival, oxidative stress, angiogenesis, inflammation, and fibrosis (Hamming et al., 2004; Rabelo et al., 2011; Uhal et al., 2011). The first report on the brain expression of ACE2 was from tissues obtained from human autopsies (Harmer et al., 2002).

Initially, ACE2 was thought to be present only in brain endothelial and smooth muscle cells (Hamming et al., 2004), albeit animal studies in rats showed that astrocytes also expressed ACE2 (Gallagher et al., 2006). In another study, neuron-specific expression of ACE2 was reported (Doobay et al., 2007). Recent studies in human and mouse neuroblastoma, glioblastoma, and microglial cell lines have also shown that ACE2 is expressed in all these cell lines at both RNA and protein levels (Qiao et al., 2020).

ACE2 is the receptor for the severe acute respiratory syndrome coronavirus (SARS-CoV) (Li et al., 2003) and for SARS-CoV-2 (Lan et al., 2020; Lu et al., 2020). In a recent bioinformatic study, it was deduced that the spike protein in SARS-CoV-2 binds more tightly to ACE2 than that of SARS-CoV, thus increasing the potential of SARS-CoV-2 to infect brain cells expressing ACE2 (Hassanzadeh et al., 2020). Moreover, coronaviruses can enter the brain and infect human neurons and glial cells (Arbour et al., 2000, Cheng et al., 2020), and evidence of CNS coronavirus infection has been found in neural cells and cerebrospinal fluid (CSF) of COVID-19 patients (Arbour et al., 2000; Cheng et al., 2020; Karvigh et al., 2021; Song et al., 2021). All these observations, amidst the complexity of COVID-19, suggest that the regulation of ACE2 itself could play a crucial role in COVID-19 pathophysiology, including neurological symptoms, complications and sequalae.
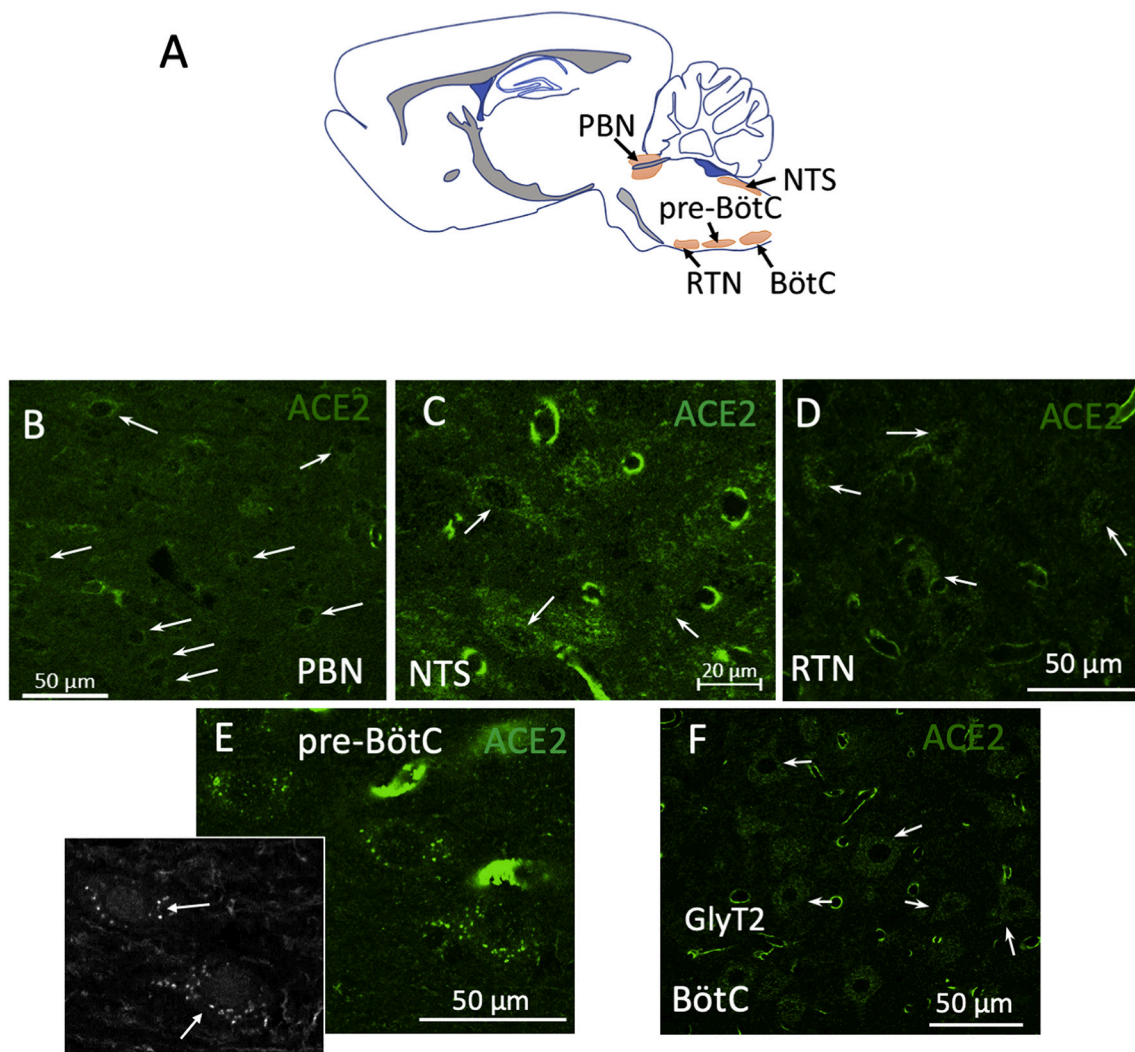
Fig. 3. ACE2 is highly expressed in nuclei of the brainstem respiratory network. A: Schematic representation of the pontomedullary nuclei involved in breathing control, where high numbers of ACE2 expressing non-endothelial cells were found. B-F: High power confocal photomicrographs of the parabrachial nucleus (PBN), the nucleus of tractus solitarius (NTS), retrotrapezoid nucleus (RTN), pre-Bötzinger complex (pre-BötC), and Bötzinger complex (BötC). Inset in panel E shows the colocalization of the glycine transporter 2 in glycinergic neurons of the pre-BötC. Arrows in all panels indicate some of the observed ACE2 positive cells.

4.1. ACE2 in the blood-brain barrier cellular components

The blood-brain barrier (BBB) is crucial to maintain an adequate milieu for the normal physiological activity of neurons in different brain areas. It comprises a continuous, non-fenestrated endothelium and the accessory peri-endothelial structures as pericytes, astrocytes, and a thin basement membrane (Reese and Karnovsky, 1967). Endothelial cells, through tight junctions, seal the paracellular space, restricting the passage of substances to transport mediated by transporters or transcytosis. In the peri-endothelial space, astrocytes and pericytes regulate capillary flow and transcytosis (Armulik et al., 2010; Segarra et al., 2021).

In this study, we showed that the density and distribution of immunopositive vasculature were heterogeneous between brain areas, with the highest density in the olfactory bulb, the supraoptic and paraventricular nuclei, and the mammillary bodies of the hypothalamus, the midbrain dopaminergic substantia nigra, and ventral tegmental area, and nuclei in the pons and medulla involved in the regulation of breathing and arousal (Table2). Through immunofluorescence, we reported the expression of ACE2 in the cytoplasm of astrocytes, which are key components of the BBB. Notably, we noted that the endfoot processes of these cells were surrounding blood vessels (Fig. 2) and had close contact with neurons (Fig. 7), suggesting a possible route for neuronal infection. The other cells of the BBB are the pericytes and the endothelial cells, we found that ACE2 was expressed in all pericytes and some endothelial cells.

Recent histopathological studies from patients who died from severe COVID-19 indicate the presence of endothelial inflammation at gray matter structures (Kirschenbaum et al., 2021). Neuroinflammatory abnormalities during COVID-19 could be partially explained based on changes in ACE2 expression at the BBB of the vast brain network of capillaries, which could affect the integrity of endothelial tight junctions allowing passage of cytokines and inflammatory cells into the brain. The diffusion of SARS-CoV-2 directly to nervous tissue and/or by infiltration of infected lymphocytes to the perivascular space would leave glia and neurons directly exposed to the virus. Furthermore, cytokines might cause abnormalities in the excitability of neurons by affecting neurotransmitter release, cell survival, and synaptic integrity in certain brain circuits, resulting in functional abnormalities (Vezzani and Viviani, 2015).

It has been increasingly recognized that alterations in the normal brain hemodynamics are a common feature of COVID-19 and vascular events such as stroke are frequent (Kakarla et al., 2021; Sashindranath and Nandurkar, 2021). Some imaging studies have shown alterations in cerebral blood flow in patients with COVID-19 (Sonkaya et al., 2020). And even in patients with no overt neurological manifestations, there are persistent alterations in the cerebral blood flow (Qin et al., 2021). The results we present in this study on the vascular distribution of ACE2 in the brain, point out potential regions where the presence of high levels of ACE2 in the vasculature might serve as a docking point for SARS-CoV-2 entry into the brain.

4.2. ACE2 in neuronal circuits

High-throughput single-cell polymerase chain reaction and microarray studies have suggested the identity of cells or brain regions expressing ACE2 (Fodoulian et al., 2020; Lukiw et al., 2020; Muus, Luecken et al., 2021). However, little has been reported regarding the cellular identity of neurons expressing ACE2 or about the circuits where those neurons participate.

Here, we report that ACE2 is expressed in discrete neuronal groups throughout the brain, from the brainstem to the olfactory cortex. These neurons have a chemical signature that, if altered, might cause functional abnormalities at different levels and thus, explain some of the clinical manifestations of COVID-19. In the following sections, we analyze the possible role of ACE2 expressing neurons in various circuits and the possible pathophysiological consequences of its disbalance in relevant physiological circuits.

4.2.1. Circuits for respiratory control and arousal

Several nuclei involved in breathing and sleep-wake transitions are in the rhombencephalon, between the pons and medulla. The neurons responsible for modulating breathing can be largely found in three groups of nuclei located in the pons and the ventrolateral and dorsolateral medulla. These nuclei are involved in the unconscious control of breathing by controlling the contraction and relaxation of respiratory muscles in response to signals from chemoreceptors that sense oxygen or carbon monoxide concentration in the blood (Dutschmann and Dick, 2012). The pontine respiratory group is constituted by neurons in the
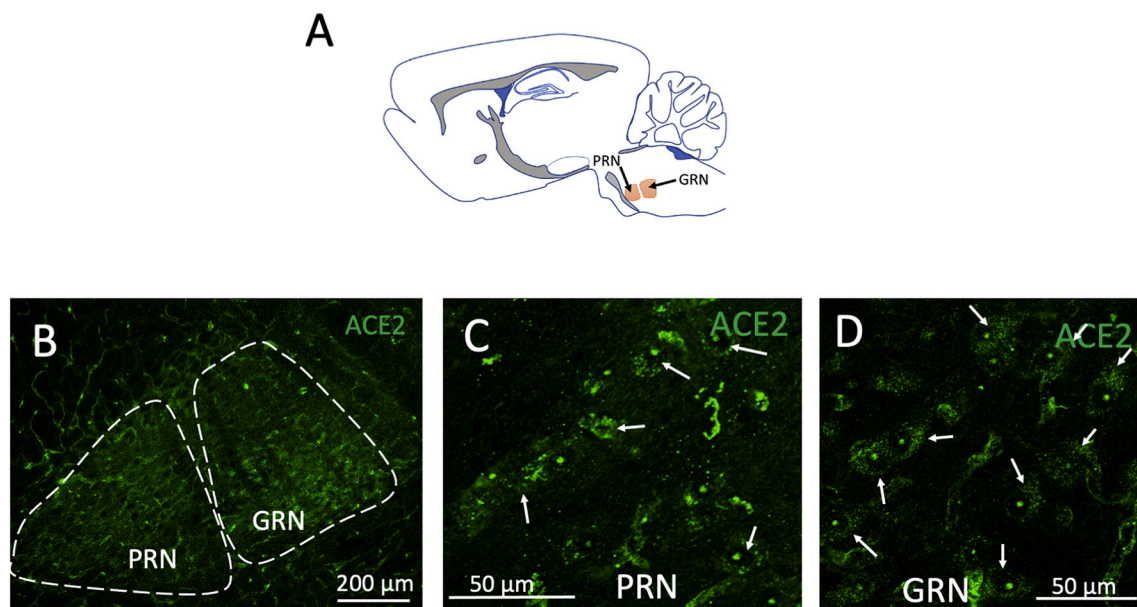

Fig. 4. ACE2 is highly expressed in arousal-related reticular formation pontomedullary nuclei. A: Schematic representation of the location of the pontine reticular nuclei (PRN) and gigantocellular reticular nucleus (GRN) in a sagittal section. Low power (B) and high power (C and D) confocal photomicrographs show ACE2 positive cells identified in PRN. Arrows indicate examples of some of those cells.
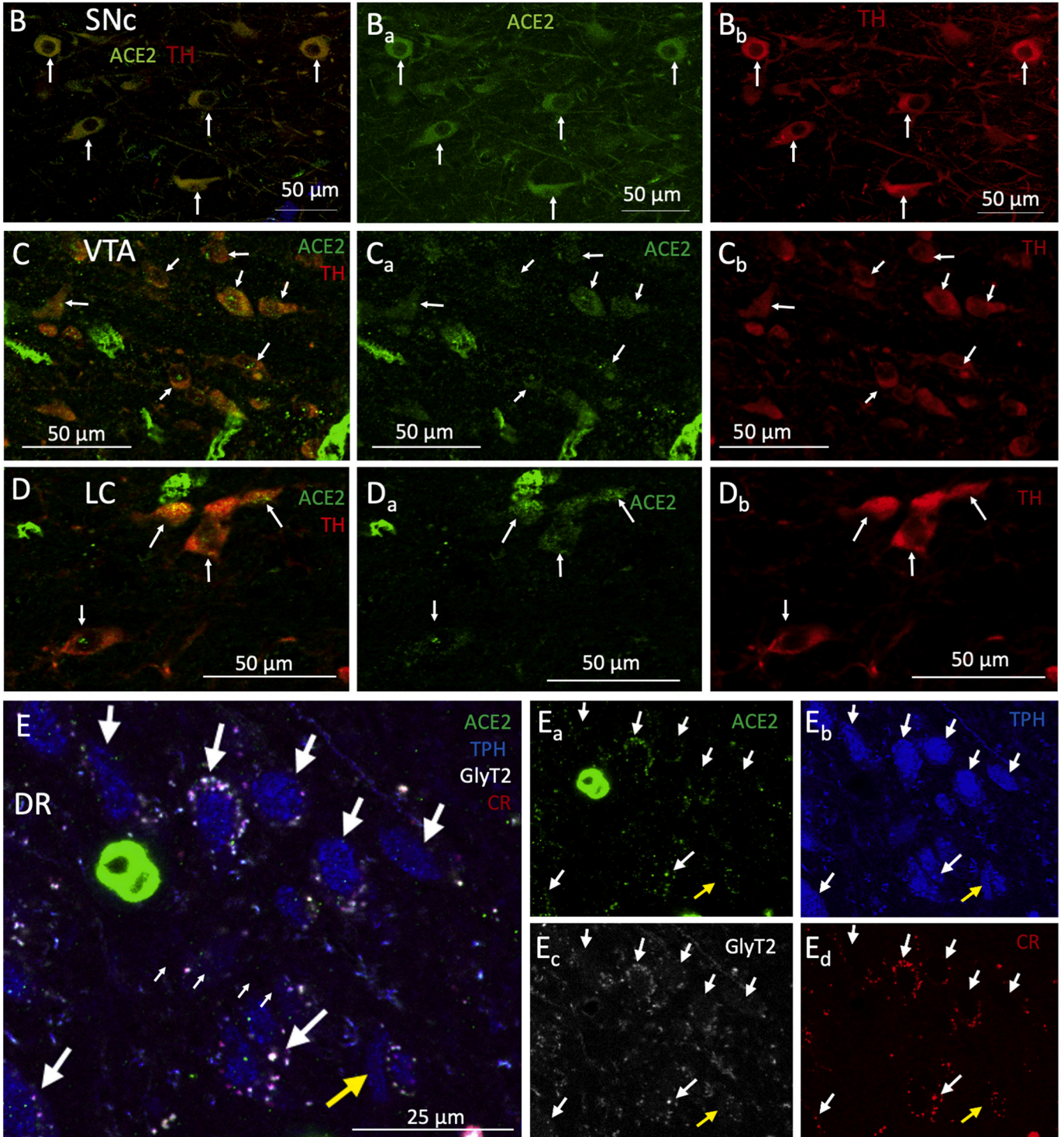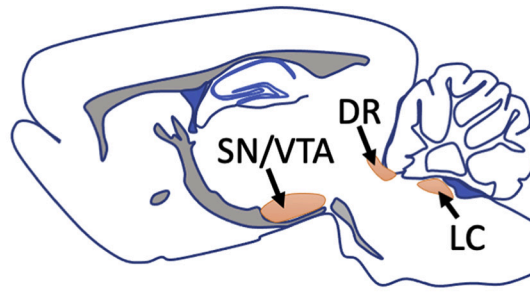
(caption on next page)

Fig. 5. ACE2 is expressed in brainstem aminergic nuclei. A) Schematic representation of the evaluated brainstem aminergic nuclei location in a sagittal section. B - D) ACE2 is expressed in tyrosine hydroxylase (TH) expressing neurons within the substantia nigra pars compacta (SNc, panel B) and ventral tegmental area (VTA, panel C) dopaminergic regions, as well as in the locus coeruleus (LC, panel D) noradrenergic region. E) Many tryptophan hydroxylase (TPH) neurons in the serotoninergic dorsal raphe (DR) nucleus were positive for ACE2 and co-expressed the glycine transporter 2 (GlyT2) and the calcium-binding protein calretinin (CR). Sparse TPH-positive neurons (indicated by the yellow arrow) do not express ACE2, CR, nor GlyT2. (For interpretation of the references to colour in this figure legend, the reader is referred to the web version of this article.)

parabrachial complex. Neurons in this group have been shown to project onto phrenic motoneurons. They receive important sensory input from the nucleus of *tractus solitarius* (NTS) and chemoreceptor information from the RTN / PF nuclei. The activation of this nucleus causes abrupt cessation of inspiration, and it has been implicated in resetting the respiratory rhythm in response to sensory stimuli. Lesions to these nuclei inhibit the tachypnea induced by hypoxia or hypercapnia. The dorsal medullary group consists of neurons located in the NTS. At least two types of neurons have been identified; one type is presynaptic to phrenic motoneurons, the second type has been shown to receive input from stretch receptors in the lung and send outputs to other groups in the respiratory network (Bautista et al., 2014). The ventral medullary

respiratory group consists of the RNT/PFZ nuclei, the pre-Bötzinger complex, and the Bötzinger complex. The RTN/PFZ has been shown to contain PHOX2B-positive neurons able to sense CO2 concentrations (Onimaru et al., 2014). This area also receives information about oxygen levels from the carotid bodies (Guyenet et al., 2019). Mutations in PHOX2B are associated with a syndrome of congenital hypoventilation in humans (Amiel et al., 2003). The Bötzinger complex has mainly an expiratory function with the adjacent pre-Bötzinger complex involved mainly in the inspiratory phase of breathing (Smith et al., 2009). The Bötzinger complex contains a large population of glycinergic neurons (Winter et al., 2009). The presence of angiotensin II in the respiratory network was noted in the late eighties by Aguirre et al. They reported a
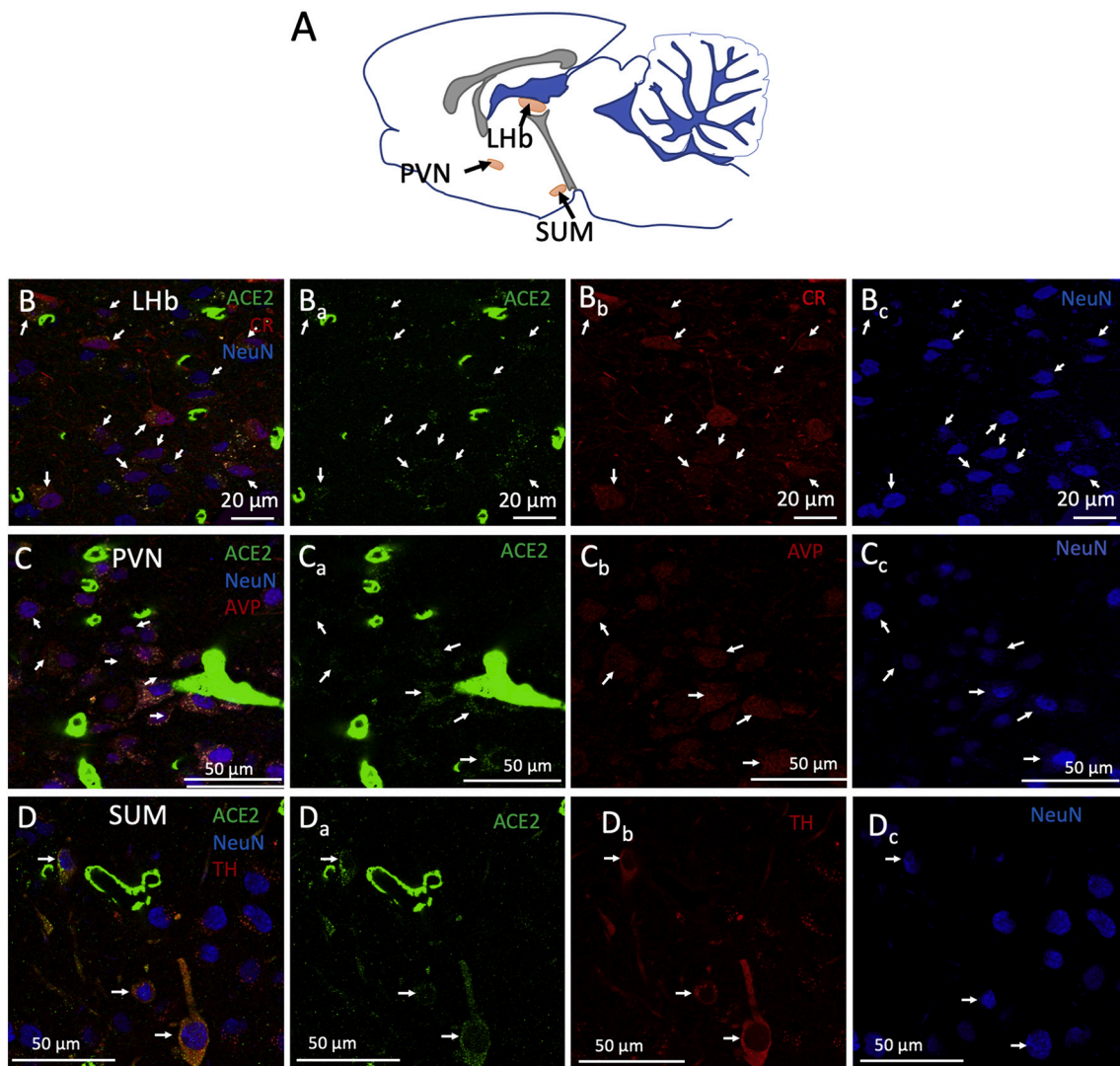
Fig. 6. ACE2 is expressed in the diencephalic lateral habenula, paraventricular and supramammillary neurons. A) Schematic representation in a sagittal slice, of the lateral habenula (LHb), paraventricular nucleus (PVN), and supramammillary nucleus (SUM), where some neurons expressing ACE2 were characterized. B) Confocal photomicrograph showing (arrows) that ACE2 is expressed in calretinin (CR) positive neurons (NeuN, Neuron-Specific Nuclear Protein). B) Arrows in photomicrographs show the colocalization of ACE2 in vasopressinergic (AVP) positive neurons (NeuN). D) In the SUM, we found tyrosine hydroxylase (TH) positive neurons (NeuN) that co-express ACE2. Other non-TH neurons did not express ACE2.

cluster of angiotensin II immunopositive somata in the Bötzinger complex and Parabrachial nucleus and abundant immunopositive fibers in the nucleus tractus solitarius (NTS) and medial PBN (Aguirre et al., 1989). However, the exact chemosensory mechanism of this process remained elusive. A recent study used a microarray design to quantify the expression of ACE2 RNA in some samples of human brain autopsies; the results showed that the most intense expression of ACE2 was in the medulla and pons. In this study, we report a large group of neurons located in different dorsal and ventral nuclei of the respiratory complex that are ACE2 immunopositive (Fig. 3). In the pontine respiratory group, we found ACE2 expression in neurons of the parabrachial nucleus (PBN). From the ventral respiratory group, ACE2 was expressed in neurons of the retrotrapezoid nucleus (RTN), in the glycinergic transporter (GlyT2) expressing neurons of the pre-Bötzinger complex (PreBötC), and in the Bötzinger complex (BötC). From the dorsal respiratory group, we found ACE2 positive cells in NTS. From the reticular formation, ACE2 positive

cells were identified in the caudal pontine reticular nucleus (PRN) and gigantocellular reticular nucleus (GRN) (Fig. 3).

One of the main symptoms of COVID-19 patients is the lack of perception of dangerously low levels of blood oxygen, a phenomenon called "happy hypoxemia" or silent hypoxemia (U and Verma, 2020). Also of great concern is the high incidence of patients unable to restore their normal autonomic ventilation after being under artificially controlled ventilation. A possible hypothesis to explain these observations is that SARS-CoV-2 exerts cytotoxic effects on the infected cells of the respiratory network. This damage could impede the restoration of normal ventilatory rhythmicity or affect chemosensation of CO_2 and O_2 levels in the blood, thus inhibiting the perception of dangerous levels of hypoxia or hypercapnia. A final possibility to explain the ventilatory anomalies observed in COVID-19 patients, is that infection of ACE2-expressing cells downregulates expression of the latter, reducing the transformation of angiotensin II to angiotensin I. Excessive angiotensin
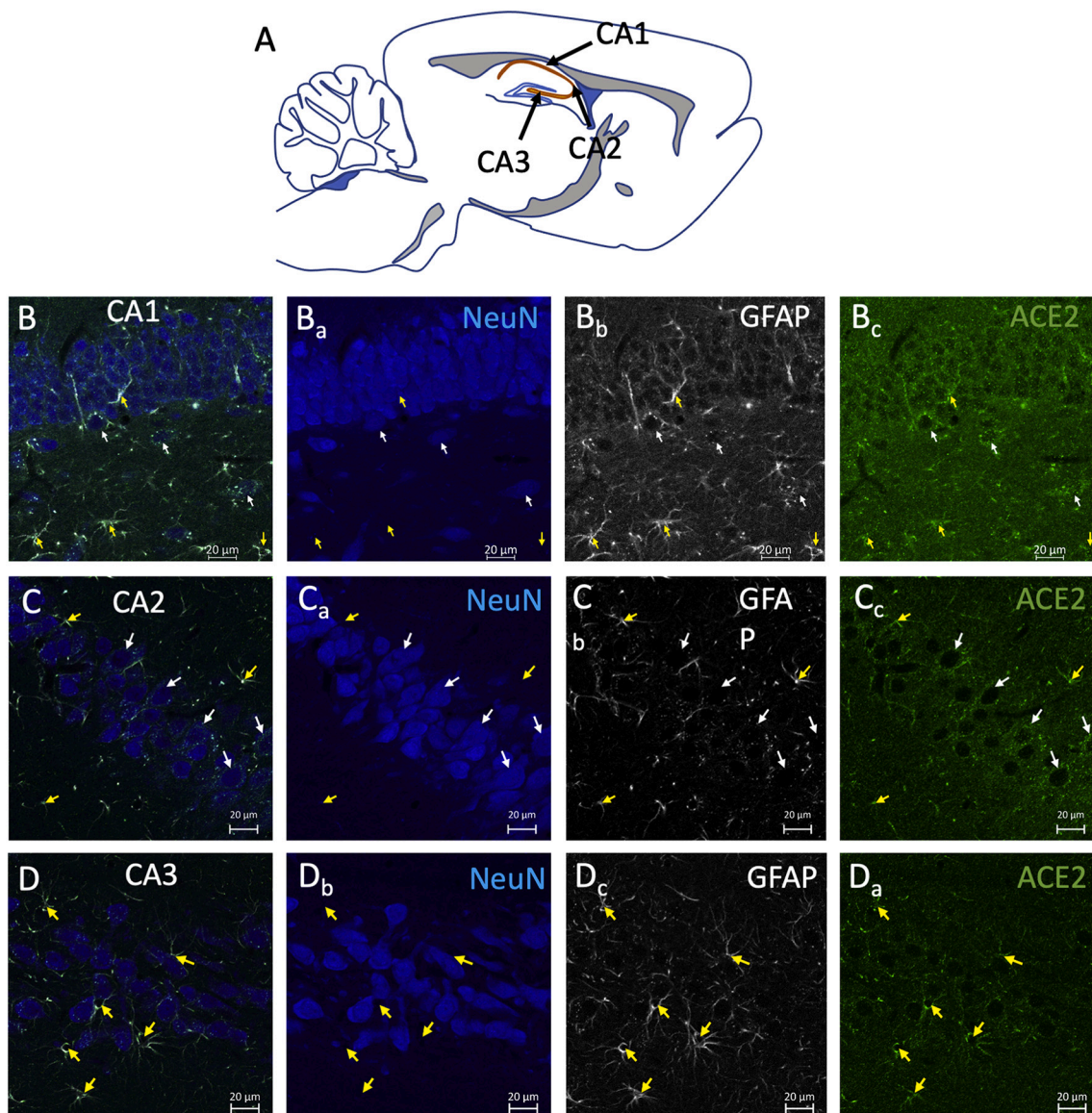
Fig. 7. ACE2 is expressed in neurons and astrocytes in the hippocampus. A) Schematic representation of a sagittal brain slice, indicating the location of the CA (Cornu Ammonis) fields of the hippocampus in orange colour, where the high-power photomicrographs of the following panels were taken. B—D) Confocal photomicrographs in the regions of CA1 (panels Bs), CA2 (Panels Cs), and CA3 (Panels Ds), showing neurons that were double-labeled with ACE2 and NeuN (white arrows) or astrocytes labeled with ACE2 and GFAP (yellow arrows). Note the presence of the GFAP+ /ACE+ astrocytic processes projecting into the pyramidal layer. Also, notice that the ACE2 positive neurons were mainly outside the pyramidal layer. (For interpretation of the references to colour in this figure legend, the reader is referred to the web version of this article.)
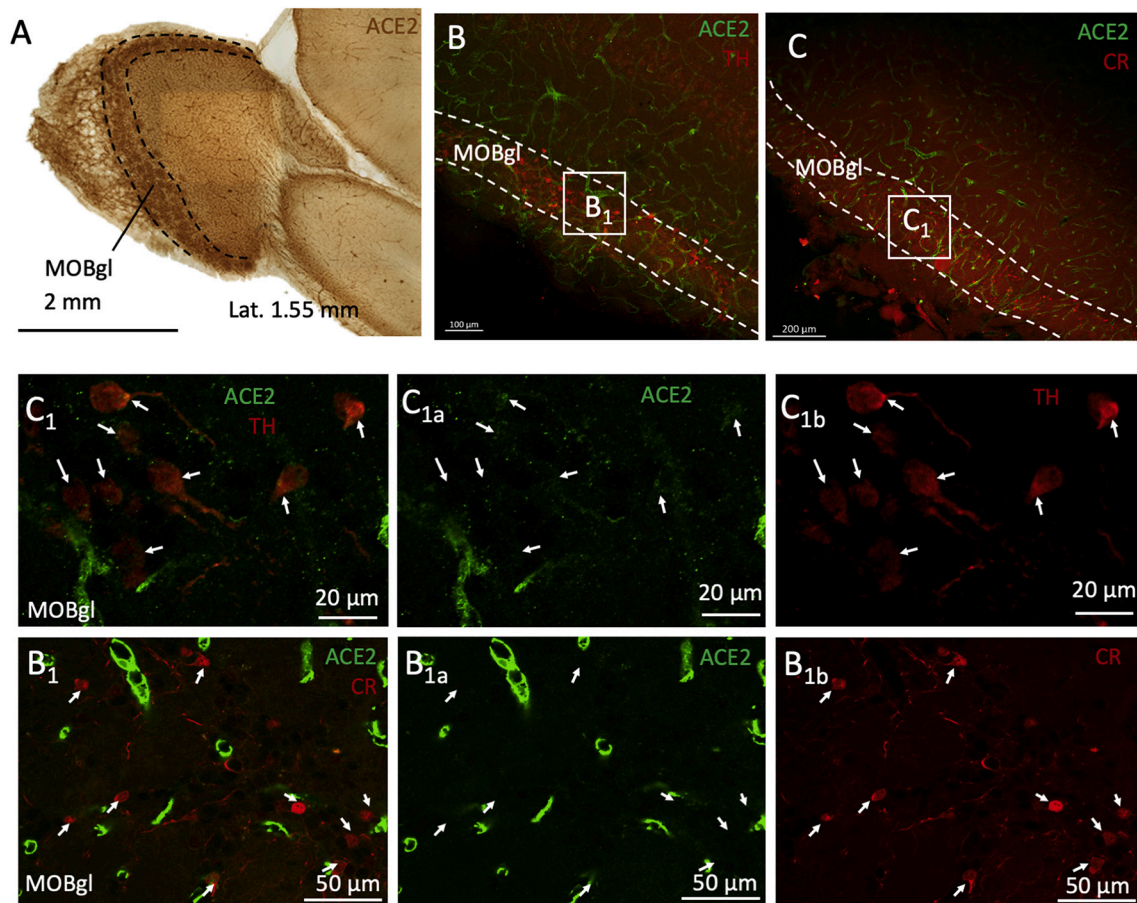
Fig. 8. ACE2 is expressed in TH positive neurons of the main olfactory bulb (MOB). A) Low magnification photomicrograph of a DAB developed immunoreaction against ACE2 in the olfactory bulb region at the lateral 1.4 mm coordinate. The highest expression of ACE2 was found in the glomerular layer (MOBgl). Panels B and C show low-power confocal photomicrographs of sections double-labeled against ACE2 and calretinin (CR, panel B) or tyrosine hydroxylase (TH, panel C). High-power photomicrographs of the squared regions labeled as B_1 and C_1 are shown in the lower panels. ACE2 positive neurons were negative for CR (panel B_{1s}) in the glomerular layer but positive for TH (panel C_{1s}).

II could affect the function of circuits involved in breathing control. In support of this hypothesis, an association between genetic variation in ACE activity, and fatal cardiorespiratory pathology, has been reported (Harding et al., 2003).

4.2.2. Circuits for hydroelectrolytic homeostasis

The paraventricular (PVN) and supraoptic (SON) nuclei of the hypothalamus are crucial to regulating blood volume and osmolarity (Dunn et al., 1973). However, these nuclei also innervate central targets in limbic and brainstem regions such as the hippocampus, amygdala, habenula, and locus coeruleus and modulate behavioral cognitive and emotional responses (Cui et al., 2013, Zhang and Hernandez, 2013, Hernandez et al., 2015, Hernandez et al., 2016, Zhang et al., 2016).

We found that PVN and SON are richly vascularized structures in the brain with high ACE2 expression. Any vascular disruption would necessarily affect the normal functioning of those nuclei. Moreover, we found ACE2 expression in vasopressinergic neurons, confirming previous reports using transcriptomic analysis (Nampoothiri et al., 2020). It is known that the RAAS regulates the secretion of vasopressin, particularly, angiotensin II stimulates the release of vasopressin (Sandgren et al., 2018). Mice overexpressing ACE2 showed a diminished hypertensive response to the systemic administration of angiotensin II (Feng et al., 2012) and reduced deoxycorticosterone acetate (DOCA)-salt-induced hypertension (Xia et al., 2015). Also, pharmacological interventions that increase ACE2 expression in the brain have been shown to produce antihypertensive effects and decrease vasopressin release

(Hmazzou et al., 2021). A series of case reports have noted the presence of syndrome of inadequate antidiuretic hormone secretion (SIADH) in COVID-19 (Yousaf et al., 2020). Current literature suggests that the increase in vasopressin seen in some patients with COVID-19 is mediated by systemic inflammation, which acts as a non-osmotic stimulus for vasopressin production (Swart et al., 2011) and kidney damage (Gheorghe et al., 2021). However, it could be argued that SARS-CoV2 directly invades the BBB components of the highly vascularized PVN and SON, thus causing significant disruption in homeostasis that leads to altered hormonal secretion and consequently, SIADH, or that the direct infection of AVP producing neurons by SARS-CoV-2 leads to an internalization of its receptor (ACE2) and subsequent accumulation of the hormone angiotensin II stimulatory for AVP-release.

4.2.3. Circuits for reward, motivation, and movement

The two main dopaminergic populations of the midbrain are the ventral tegmental area (VTA), and the *sustantia nigra pars compacta* (SNpc). Three main pathways arise from these structures. The ascending projections from the VTA to the nucleus accumbens are called the mesolimbic pathway and have classically been described as part of a reward system (Wise, 1978; Schultz, 2002). The projections from VTA to the prefrontal cortex are called the mesocortical pathway and are associated with modulation of cognitive, working memory, and decision-making functions (Tanaka, 2006; Lapish et al., 2007; Verharen et al., 2018). Finally, the nigrostriatal pathway arises in the SN and terminates in the caudate and putamen. It has been associated with the

modulation of voluntary movement (Smith and Bolam, 1990; Prensa et al., 2009). These circuits are modulated by excitatory projections from the lateral habenula (LHb) via an inhibitory relay in the tail of the VTA (Barrot et al., 2012; Bourdy and Barrot, 2012; Stamatakis and Stuber, 2012). This study found ACE2/tyrosine hydroxylase (TH) co-expressing neurons in both VTA and SNpc.

The dorsal raphe nucleus (DRN) hosts the largest group of serotoninergic neurons and has classically been implicated in the modulation of mood. Studies have shown alterations in the anatomy or function of this nucleus in depression or anxiety and suicide patients (Underwood et al., 1999; Bruschetta et al., 2020; Li et al., 2020). This nucleus also participates in modulating the core respiratory networks of the brainstem (Bautista et al., 2014). The lateral habenula has reciprocal connections with the DRN and is a critical modulator of the activity of serotoninergic neurons. This LHb-DRN circuit has been implicated in regulating cognition, reward, and arousal functions (Zhao et al., 2015). This study found ACE2/tryptophan hydroxylase (TPH) co-expressing neurons in the DRN with some also co-expressing the GlyT2 (a significant population of projection neurons from the DRN) (Krzywkowski et al., 1995).

Interactions between brain-*RAAS* (McKinley et al., 2003; Huang and Leenen, 2009; Cosarderelioglu et al., 2020) and the dopaminergic system have been reported. The angiotensin II infusion in the striatum provokes local dopamine release (Brown et al., 1996). Angiotensin II has been shown to regulate the synthesis of the enzymes involved in catecholamine biosynthesis (Aschrafi et al., 2019). Moreover, ACE2 has been reported in the mitochondria isolated from cell cultures derived from dopaminergic neurons (Costa-Besada et al., 2018). It is generally considered that SARS-CoV-2 induces downregulation of its receptor (Kuba et al., 2005; Peiro and Moncada, 2020; Verdecchia et al., 2020; Zhang et al., 2021). Diminishing the activity of ACE2 would lead to the accumulation of angiotensin II and possibly leading to a dysregulation of dopaminergic and serotoninergic neurons expressing ACE2. This might partly explain emotional, cognitive, motivational, and locomotor symptoms observed in COVID-19. Moreover, the increased incidence of Parkinson's disease and parkinsonism reported in the recent literature (Helmich and Bloem, 2020; Leta et al., 2021; Morassi et al., 2021) could be related to the above catecholamine metabolic dysfunction.

4.2.4. Circuits for sensory processing

In this work, we found ACE2 expression in the glomerular layer of the main olfactory bulb (MOBgl). The enzyme was present in TH positive neurons but not in calretinin positive neurons (Fig. 8). The olfactory bulb contains the largest population of dopaminergic neurons in the rat brain. Those neurons have been identified mainly as periglomerular and playing a role in the codification of the olfactory processing (Pignatelli and Belluzzi, 2017; Kosaka et al., 2020). Also, ACE2 neurons were observed in the nucleus of the tractus solitarius (NTS) and the upstream nuclei in the gustatory pathway, the parabrachial nucleus (PBN). Besides their role in processing taste information, these nuclei, as discussed above, also participate in processing chemosensory information related to the sensing of oxygen and CO2 levels. One of the most classic symptoms of COVID-19 is the loss of taste and smell (Butowt and von Bartheld, 2020; Mao et al., 2020). It may be possible that dysfunction of ACE2 expressing neurons in these sensorial circuits underly the anosmia and ageusia observed in the acute phase of the disease, and that long-lasting changes in these circuits might explain the protracted alterations that some patients report after recovery (Marshall, 2021).

The distribution of ACE2 in neuronal, astrocytic, and epithelial cells of the mammalian central nervous system, especially the evidence for heterogeneity in the abundance of expression throughout the brain, provides a template for understanding neurological manifestations of SARS-CoV-2 infection both during infection and following viral clearance. Since ACE2 is the receptor of SARS-CoV (Li et al., 2003) and SARS-CoV-2 (Lan et al., 2020; Lu et al., 2020) and also has a role in maintaining a normal brain function (Xu et al., 2011), it is feasible to

hypothesize two possible pathophysiological mechanisms for the clinical manifestations of COVID-19 and the post-acute COVID-19 syndrome. First, ACE2 functions as a high affinity receptor (Hassanzadeh et al., 2020) for the entry of the virus to different neural populations and for the selective neurotropic invasion and damage/death to given neural circuits. Secondly, reductions in the abundance of ACE2 induced by the binding of the virus (Kuba et al., 2005; Dijkman et al., 2012), induce modifications on the local concentration of peptidergic substrates or prioducts of this enzyme (Zhang et al., 2021). Both processes could be of importance for the COVID induced neuropathology and merit urgent further investigation.

Declaration of Competing Interests

The authors declare that they have no known competing financial interests or personal relationships that could have appeared to influence the work reported in this paper.

References

Aguirre, J.A., Covenas, R., Croix, D., Alonso, J.R., Narvaez, J.A., Tramu, G., Gonzalez-Baron, S., 1989. Immunocytochemical study of angiotensin-II fibres and cell bodies in the brainstem respiratory areas of the cat. Brain Res. 489 (2), 311–317.

Amiel, J., Laudier, B., Attie-Bitach, T., Trang, H., de Pontual, L., Gener, B., Trochet, D., Etchevers, H., Ray, P., Simonneau, M., Vekemans, M., Munnich, A., Gaultier, C., Lyonnet, S., 2003. Polyalanine expansion and frameshift mutations of the paired-like homeobox gene PHOX2B in congenital central hypoventilation syndrome. Nat. Genet. 33 (4), 459–461.

Arbour, N., Day, R., Newcombe, J., Talbot, P.J., 2000. Neuroinvasion by human respiratory coronaviruses. J. Virol. 74 (19), 8913–8921.

Armulik, A., Genove, G., Mae, M., Nisancioglu, M.H., Wallgard, E., Niaudet, C., He, L., Norlin, J., Lindblom, P., Strittmatter, K., Johansson, B.R., Betsholtz, C., 2010. Pericytes regulate the blood-brain barrier. Nature 468 (7323), 557–561.

Aschrafi, A., Berndt, A., Kowalak, J.A., Gale, J.R., Gioio, A.E., Kaplan, B.B., 2019. Angiotensin II mediates the axonal trafficking of tyrosine hydroxylase and dopamine beta-hydroxylase mRNAs and enhances norepinephrine synthesis in primary sympathetic neurons. J. Neurochem. 150 (6), 666–677.

Barrot, M., Sesack, S.R., Georges, F., Pistis, M., Hong, S., Jhou, T.C., 2012. Braking dopamine systems: a new GABA master structure for mesolimbic and nigrostriatal functions. J. Neurosci. 32 (41), 14094–14101.

Bautista, T.G., Pitts, T.E., Pilowsky, P.M., Morris, K.F., 2014. Chapter 18 - The Brainstem Respiratory Network. In: Faingold, C.L., Blumenfeld, H. (Eds.), Neuronal Networks in Brain Function, CNS Disorders, and Therapeutics. Academic Press, San Diego, pp. 235–245.

Bourdy, R., Barrot, M., 2012. A new control center for dopaminergic systems: pulling the VTA by the tail. Trends Neurosci. 35 (11), 681–690.

Brown, D.C., Steward, L.J., Ge, J., Barnes, N.M., 1996. Ability of angiotensin II to modulate striatal dopamine release via the AT1 receptor in vitro and in vivo. Br. J. Pharmacol. 118 (2), 414–420.

Bruschetta, G., Jin, S., Liu, Z.W., Kim, J.D., Diano, S., 2020. MC4R signaling in dorsal raphe nucleus controls feeding, anxiety, and depression. Cell Rep. 33 (2), 108267.

Butowt, R., von Bartheld, C.S., 2020. Anosmia in COVID-19: underlying mechanisms and assessment of an olfactory route to brain infection. Neuroscientist. https://doi.org/10.1177/1073858420956905.

Cheng, Q., Yang, Y., Gao, J., 2020. Infectivity of human coronavirus in the brain. EBioMedicine 56, 102799.

Cohen, M.E., Eichel, R., Steiner-Birmanns, B., Janah, A., Ioshpa, M., Bar-Shalom, R., Paul, J.J., Gaber, H., Skrahina, V., Bornstein, N.M., Yahalom, G., 2020. A case of probable Parkinson's disease after SARS-CoV-2 infection. Lancet Neurol. 19 (10), 804–805.

Cosarderelioglu, C., Nidadavolu, L.S., George, C.J., Oh, E.S., Bennett, D.A., Walston, J.D., Abadir, P.M., 2020. Brain renin-angiotensin system at the intersect of physical and cognitive frailty. Front. Neurosci. 14, 586314.

Costa-Besada, M.A., Valenzuela, R., Garrido-Gil, P., Villar-Cheda, B., Parga, J.A., Lanciego, J.L., Labandeira-Garcia, J.L., 2018. Paracrine and intracrine angiotensin 1-7/mas receptor axis in the substantia Nigra of rodents, monkeys, and humans. Mol. Neurobiol. 55 (7), 5847–5867.

Peiro, C., Moncada, S., 2020. Substituting angiotensin-(1-7) to prevent lung damage in SARS-CoV-2 infection? Circulation 141 (21), 1665–1666.

Pignatelli, A., Belluzzi, O., 2017. Dopaminergic neurones in the main olfactory bulb: an overview from an electrophysiological perspective. Front. Neuroanat. 11, 7.

Prensa, L., Gimenez-Amaya, J.M., Parent, A., Bernacer, J., Cebrian, C., 2009. The nigrostriatal pathway: axonal collateralization and compartmental specificity. J. Neural Transm. Suppl. 73, 49–58.

Qiao, J., Li, W., Bao, J., Peng, Q., Wen, D., Wang, J., Sun, B., 2020. The expression of SARS-CoV-2 receptor ACE2 and CD147, and protease TMPRSS2 in human and mouse brain cells and mouse brain tissues. Biochem. Biophys. Res. Commun. 533 (4), 867–871.

Qin, Y., Wu, J., Chen, T., Li, J., Zhang, G., Wu, D., Zhou, Y., Zheng, N., Cai, A., Ning, Q., Manyande, A., Xu, F., Wang, J., Zhu, W., 2021. Long-term micro-structure and cerebral blood flow changes in patients recovered from COVID-19 without neurological manifestations. J. Clin. Invest. https://doi.org/10.1172/JCI147329.

Rabelo, L.A., Alenina, N., Bader, M., 2011. ACE2-angiotensin-(1-7)-Mas axis and oxidative stress in cardiovascular disease. Hypertens. Res. 34 (2), 154–160.

Rahman, M.A., Islam, K., Rahman, S., Alamin, M., 2021. Neurobiochemical cross-talk between COVID-19 and Alzheimer's disease. Mol. Neurobiol. 58 (3), 1017–1023.

Reese, T.S., Karnovsky, M.J., 1967. Fine structural localization of a blood-brain barrier to exogenous peroxidase. J. Cell Biol. 34 (1), 207–217.

Rice, G.I., Thomas, D.A., Grant, P.J., Turner, A.J., Hooper, N.M., 2004. Evaluation of angiotensin-converting enzyme (ACE), its homologue ACE2 and neprilysin in angiotensin peptide metabolism. Biochem. J. 383 (Pt 1), 45–51.

Sandgren, J.A., Linggonegoro, D.W., Zhang, S.Y., Sapouckey, S.A., Claflin, K.E., Pearson, N.A., Leidinger, M.R., Pierce, G.L., Santillan, M.K., Gibson-Corley, K.N., Sigmund, C.D., Grobe, J.L., 2018. Angiotensin AT1A receptors expressed in vasopressin-producing cells of the supraoptic nucleus contribute to osmotic control of vasopressin. Am. J. Phys. Regul. Integr. Comp. Phys. 314 (6), R770–R780.

Sashindranath, M., Nandurkar, H.H., 2021. Endothelial dysfunction in the brain: setting the stage for stroke and other cerebrovascular complications of COVID-19. Stroke 52 (5), 1895–1904.

Satarker, S., Nampoothiri, M., 2020. Involvement of the nervous system in COVID-19: the bell should toll in the brain. Life Sci. 262, 118568.

Schultz, W., 2002. Getting formal with dopamine and reward. Neuron 36 (2), 241–263.

Segarra, M., Aburto, M.R., Acker-Palmer, A., 2021. Blood-brain barrier dynamics to maintain brain homeostasis. Trends Neurosci. 44 (5), 393–405.

Smith, A.D., Bolam, J.P., 1990. The neural network of the basal ganglia as revealed by the study of synaptic connections of identified neurones. Trends Neurosci. 13 (7), 259–265.

Smith, J.C., Abdala, A.P., Rybak, I.A., Paton, J.F., 2009. Structural and functional architecture of respiratory networks in the mammalian brainstem. Philos. Trans. R. Soc. Lond. Ser. B Biol. Sci. 364 (1529), 2577–2587.

Song, E., Zhang, C., Israelow, B., Lu-Culligan, A., Prado, A.V., Skriabine, S., Lu, P., Weizman, O.E., Liu, F., Dai, Y., Szigeti-Buck, K., Yasumoto, Y., Wang, G., Castaldi, C., Heltke, J., Ng, E., Wheeler, J., Alfajaro, M.M., Levavasseur, E., Fontes, B., Ravindra, N.G., Van Dijk, D., Mane, S., Gunel, M., Ring, A., Kazmi, S.A.J., Zhang, K., Wilen, C.B., Horvath, T.L., Plu, I., Haik, S., Thomas, J.L., Louvi, A., Farhadian, S.F., Huttner, A., Seilhean, D., Renier, N., Bilguvar, K., Iwasaki, A., 2021. Neuroinvasion of SARS-CoV-2 in human and mouse brain. J. Exp. Med. 218 (3).

Sonkaya, A.R., OzTurk, B., Karada, S.O., 2020. Cerebral hemodynamic alterations in patients with Covid-19. Turk. J. Med. Sci. 51 (2), 435–439. https://doi.org/10.3906/sag-2006-203.

Stamatakis, A.M., Stuber, G.D., 2012. Activation of lateral habenula inputs to the ventral midbrain promotes behavioral avoidance. Nat. Neurosci. 15 (8), 1105–1107.

Stefano, G.B., Ptacek, R., Ptackova, H., Martin, A., Kream, R.M., 2021. Selective neuronal mitochondrial targeting in SARS-CoV-2 infection affects cognitive processes to induce 'Brain Fog' and results in behavioral changes that favor viral survival. Med. Sci. Monit. 27, e930886.

Swart, R.M., Hoorn, E.J., Betjes, M.G., Zietse, R., 2011. Hyponatremia and inflammation: the emerging role of interleukin-6 in osmoregulation. Nephron Physiol. 118 (2), 45–51.

Tanaka, S., 2006. Dopaminergic control of working memory and its relevance to schizophrenia: a circuit dynamics perspective. Neuroscience 139 (1), 153–171.

Tipnis, S.R., Hooper, N.M., Hyde, R., Karran, E., Christie, G., Turner, A.J., 2000. A human homolog of angiotensin-converting enzyme. Cloning and functional expression as a captopril-insensitive carboxypeptidase. J. Biol. Chem. 275 (43), 33238–33243.

U, R.A., Verma, K., 2020. Happy hypoxemia in COVID-19-aneural hypothesis. ACS Chem. Neurosci. 11 (13), 1865–1867.

Uhal, B.D., Li, X., Xue, A., Gao, X., Abdul-Hafez, A., 2011. Regulation of alveolar epithelial cell survival by the ACE-2/angiotensin 1-7/Mas axis. Am. J. Phys. Lung Cell. Mol. Phys. 301 (3), L269–L274.

Underwood, M.D., Khaibulina, A.A., Ellis, S.P., Moran, A., Rice, P.M., Mann, J.J., Arango, V., 1999. Morphometry of the dorsal raphe nucleus serotonergic neurons in suicide victims. Biol. Psychiatry 46 (4), 473–483.

Verdecchia, P., Cavallini, C., Spanevello, A., Angeli, F., 2020. The pivotal link between ACE2 deficiency and SARS-CoV-2 infection. Eur. J. Intern. Med. 76, 14–20.

Verharen, J.P.H., de Jong, J.W., Roelofs, T.J.M., Huffels, C.F.M., van Zessen, R., Luijendijk, M.C.M., Hamelink, R., Willuhn, I., den Ouden, H.E.M., van der Plasse, G., Adan, R.A.H., Vanderschuren, L., 2018. A neuronal mechanism underlying decision-making deficits during hyperdopaminergic states. Nat. Commun. 9 (1), 731.

Vezzani, A., Viviani, B., 2015. Neuromodulatory properties of inflammatory cytokines and their impact on neuronal excitability. Neuropharmacology 96 (Pt A), 70–82.

Vickers, C., Hales, P., Kaushik, V., Dick, L., Gavin, J., Tang, J., Godbout, K., Parsons, T., Baronas, E., Hsieh, F., Acton, S., Patane, M., Nichols, A., Tummino, P., 2002. Hydrolysis of biological peptides by human angiotensin-converting enzyme-related carboxypeptidase. J. Biol. Chem. 277 (17), 14838–14843.

Winter, S.M., Fresemann, J., Schnell, C., Oku, Y., Hirrlinger, J., Hulsmann, S., 2009. Glycinergic interneurons are functionally integrated into the inspiratory network of mouse medullary slices. Pflugers Arch. 458 (3), 459–469.

Wise, R.A., 1978. Catecholamine theories of reward: a critical review. Brain Res. 152 (2), 215–247.

Xia, H., de Queiroz, T.M., Sriramula, S., Feng, Y., Johnson, T., Mungrue, I.N., Lazartigues, E., 2015. Brain ACE2 overexpression reduces DOCA-salt hypertension independently of endoplasmic reticulum stress. Am. J. Phys. Regul. Integr. Comp. Phys. 308 (5), R370–R378.

Xu, P., Sriramula, S., Lazartigues, E., 2011. ACE2/ANG-(1-7)/Mas pathway in the brain: the axis of good. Am. J. Phys. Regul. Integr. Comp. Phys. 300 (4), R804–R817.

Yan, R., Zhang, Y., Li, Y., Xia, L., Guo, Y., Zhou, Q., 2020. Structural basis for the recognition of SARS-CoV-2 by full-length human ACE2. Science 367 (6485), 1444–1448.

Yousaf, Z., Al-Shokri, S.D., Al-Soub, H., Mohamed, M.F.H., 2020. COVID-19-associated SIADH: a clue in the times of pandemic! Am. J. Physiol. Endocrinol. Metab. 318 (6), E882–E885.

Zhang, L., Hernandez, V.S., 2013. Synaptic innervation to rat hippocampus by vasopressin-immuno-positive fibres from the hypothalamic supraoptic and paraventricular nuclei. Neuroscience 228, 139–162.

Zhang, L., Hernandez, V.S., Vazquez-Juarez, E., Chay, F.K., Barrio, R.A., 2016. Thirst is associated with suppression of Habenula output and active stress coping: is there a role for a non-canonical vasopressin-glutamate pathway? Front Neural Circuit 10, 13.

Zhang, H., Penninger, J.M., Li, Y., Zhong, N., Slutsky, A.S., 2020. Angiotensin-converting enzyme 2 (ACE2) as a SARS-CoV-2 receptor: molecular mechanisms and potential therapeutic target. Intensive Care Med. 46 (4), 586–590.

Zhang, L., Zetter, M.A., Guerra, E.C., Hernandez, V.S., Mahata, S.K., Eiden, L.E., 2021. ACE2 in the second act of COVID-19 syndrome: peptide dysregulation and possible correction with oestrogen. J. Neuroendocrinol. 33 (2), e12935.

Zhao, H., Zhang, B.L., Yang, S.J., Rusak, B., 2015. The role of lateral habenula-dorsal raphe nucleus circuits in higher brain functions and psychiatric illness. Behav. Brain Res. 277, 89–98.